

# Lawrence Berkeley National Laboratory

## Recent Work

### Title

A MICROSCOPIC METHOD FOR CALCULATING THE INTRINSIC EXCITATION OCCURRING IN NUCLEAR FISSION

### Permalink

<https://escholarship.org/uc/item/3c0747vc>

### Author

Boneh, Y.

### Publication Date

1976-12-01

RECEIVED  
LIBRARY

LBL-4374 c.1  
UC-34c  
TID-4500-R64

DOCUMENT SECTION

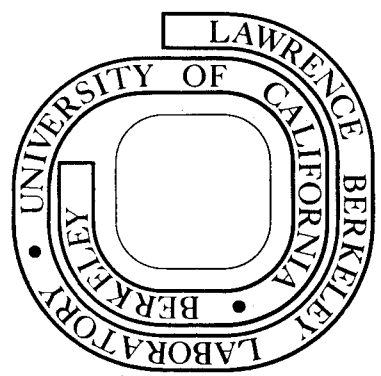
A MICROSCOPIC METHOD FOR CALCULATING THE INTRINSIC  
EXCITATION OCCURRING IN NUCLEAR FISSION

Y. Boneh, J. P. Blocki, and W. D. Myers

February 1976

Prepared for the U. S. Energy Research and  
Development Administration under Contract W-7405-ENG-48

**For Reference**  
Not to be taken from this room



LBL-4374  
c.1

0000440451

## **DISCLAIMER**

This document was prepared as an account of work sponsored by the United States Government. While this document is believed to contain correct information, neither the United States Government nor any agency thereof, nor the Regents of the University of California, nor any of their employees, makes any warranty, express or implied, or assumes any legal responsibility for the accuracy, completeness, or usefulness of any information, apparatus, product, or process disclosed, or represents that its use would not infringe privately owned rights. Reference herein to any specific commercial product, process, or service by its trade name, trademark, manufacturer, or otherwise, does not necessarily constitute or imply its endorsement, recommendation, or favoring by the United States Government or any agency thereof, or the Regents of the University of California. The views and opinions of authors expressed herein do not necessarily state or reflect those of the United States Government or any agency thereof or the Regents of the University of California.

CONTENTS

Abstract . . . . .	iv
Introduction . . . . .	1
Method of Solution . . . . .	3
Sequence of Shapes . . . . .	9
Single Particle Potential . . . . .	11
Accuracy of the Method . . . . .	12
Energies Associated with the Motion . . . . .	13
Discussion . . . . .	18
Acknowledgments . . . . .	20
Footnotes and References . . . . .	21
Figure Captions . . . . .	24

A MICROSCOPIC METHOD FOR CALCULATING THE INTRINSIC EXCITATION  
OCCURRING IN NUCLEAR FISSION\*

Y. Boneh,<sup>†</sup> J. P. Błocki<sup>‡</sup> and W. D. Myers

Nuclear Science Division  
Lawrence Berkeley Laboratory  
University of California  
Berkeley, California 94720

February 1976

ABSTRACT

A microscopic method of calculating the damping of collective motion into intrinsic excitation is described. The methods used to solve the static and time dependent Schrödinger equation are given in detail and the numerical accuracy of the method is discussed. A particular example, the excitation of neutron levels in the fission of  $^{236}\text{U}$ , is used to illustrate the approach. A number of problems are mentioned and suggestions are made as to how the work can be improved and extended.

### INTRODUCTION

One of the often observed features of atomic nuclei is the damping of large scale collective motion into intrinsic excitation.<sup>1</sup> (An excellent list of references related to the work described here is contained in Ref. 2.) The fact that dipole and quadrupole vibrations are heavily damped while rotations seem to be unaffected indicates that the damping is associated with changes in shape of the nuclear density distribution. (Low lying quadrupole vibrations in even nuclei are an exception. Such vibrations are undamped simply because their energy is so low that they lie in a region near the ground state characterized by zero single particle level density.) The evaporation of neutrons from the separating fragments in nuclear fission is another indication that collective motion has been converted to internal excitation. The origin of this energy has usually been associated with vibrations of the separating nuclei as a consequence of their deformation at scission.<sup>3</sup> This view is now being questioned because microscopic calculations<sup>2,4</sup> (like those described here) have shown that considerable internal excitation is to be expected at an earlier stage in the fission process during the descent from saddle to scission. Macroscopic considerations (based on classical kinetic theory) motivated by this work also support the conclusion that the fission process is highly damped.<sup>5-8</sup> In fact, a whole new picture of fission dynamics seems to be emerging.

While the familiar phenomena just mentioned give clear indications of the importance of nuclear damping none of them is quite so dramatic as that seen in the collisions of very heavy ions (Refs. 12-42 of our Ref. 2). The so-called "deep inelastic" processes seen in reactions such as Kr on Bi are characterized by almost total damping of the relative

motion of the colliding nuclei. The separating fragments seem to have started from rest and have only the energy gained from Coulomb repulsion.

Efforts to understand the damping of nuclear collective motion in terms of a classical hydrodynamic viscosity have not been very successful. Calculations have shown that the measured asymptotic kinetic energy release in fission<sup>9,10</sup> is only compatible with a relatively small viscosity coefficient while the "deep inelastic" processes in heavy-ion reactions seem to require a large value. Another problem is that the tangential motion seems to be weakly damped in grazing heavy-ion collisions while the radial motion is heavily damped. This seems to indicate once again that the observed damping is mainly associated with changes in shape rather than momentum transfer between parts of the nuclear fluid moving at different velocities. The idea of a hydrodynamic viscosity is also questionable on fundamental grounds. Such a damping mechanism requires that the constituent particles have a rather short mean-free-path which seems to be incompatible with the fact that many nuclear phenomena are consistent with a completely independent particle model.

One way to determine the importance of the "single-particle" damping of collective motion into intrinsic states is simply to calculate the excitation produced in a system of independent particles when the shape of the potential well is changed as a function of time. A number of such studies have been performed<sup>2,4</sup> and more are in progress.<sup>11</sup> (Current emphasis is on Time Dependent Hartree-Fock and the need for self consistency.<sup>12-14</sup>) In this paper, which is a continuation of Refs. 15 and 16, we want to describe a particularly simple approach and some preliminary applications that have been made to the fission of <sup>236</sup>U.

The method of solution of the time dependent Schrödinger equation in terms of a fixed basis is first discussed and then the sequence of shapes chosen for the potential well is described. Then we tell how the potential is generated and go on to discuss the various collective and internal excitation energies that are observed and their interpretation.

#### METHOD OF SOLUTION

The procedures used here to solve the Schrödinger equation are quite standard. Our method is the same as that which is described so well in Ref. 17. We repeat that description in the first part of this section for completeness and so that some misprints in the original reference can be corrected. We did not include either spin-orbit coupling or residual interactions of any kind in the preliminary calculations that are described here. Some discussion of the influence of residual interactions is contained in a later section.

#### The Static Part of the Schrödinger Equation

At a given time  $t = t_0$ , the static part of the Schrödinger equation for the  $i$ th single particle wave function  $\psi_i$  is:

$$\mathcal{H}_i(t = t_0) \psi_i = E_i \psi_i. \quad (1)$$

Expanding  $\psi$  in terms of a set of finite basis wave functions  $\phi_\alpha$

$$\psi_i = \sum_{\alpha=1}^N a_{\alpha}^{(i)} \phi_{\alpha} \quad (2)$$

and inserting into Eq. (1) we get:

$$\mathcal{H}_i \sum_{\alpha=1}^N a_{\alpha}^{(i)} \phi_{\alpha} = E_i \sum_{\alpha=1}^N a_{\alpha}^{(i)} \phi_{\alpha}.$$

Multiplying this equation from the left by  $\phi_{\beta}^*$  and integrating yields:

$$\sum_{\alpha} \langle \phi_{\beta} | \mathcal{H}_i | \phi_{\alpha} \rangle a_{\alpha}^{(i)} = E_i a_{\beta}^{(i)} \quad (3)$$



Equation (3) can be written in the form  $B_i a^{(i)} = E_i a^{(i)}$ , where elements of the matrix  $B_i$  are:

$$B_{\beta\alpha}^{(i)} = \langle \phi_\beta | \mathcal{H}_i | \phi_\alpha \rangle,$$

This matrix equation can be solved by numerical diagonalization of the matrix  $B_i$ . As solutions we obtain values of the energies  $E_i$  and expansion coefficients  $a_\alpha^{(i)}$ .

For basis wave functions  $\phi_\alpha$ , axially symmetric harmonic oscillator wave functions have been chosen. In cylindrical coordinates  $(\rho, z, \phi)$ :

$$\phi_\alpha = \phi_{n_z}(z) \psi_{n_\rho}^\Lambda(\rho) \chi_\Lambda(\phi) \equiv |n_z, n_\rho, \Lambda\rangle \quad (4)$$

where:

$$\phi_{n_z}(z) = (\mu\omega_z/\hbar)^{1/4} \exp(-\xi^2/2) h_{n_z}(\xi)$$

$$\psi_{n_\rho}^\Lambda(\rho) = (2\mu\omega_\perp/\hbar)^{1/2} \exp(-\eta/2) g_{n_\rho}^\Lambda(\eta)$$

$$\chi_\Lambda(\phi) = (2\pi)^{-1/2} \exp(i\Lambda\phi)$$

and:

$$\xi = (\mu\omega_z/\hbar)^{1/2} z$$

$$\eta^{1/2} = (\mu\omega_\perp/\hbar)^{1/2} \rho$$

$$h_n(\xi) = (2^n n! \pi^{1/2})^{-1/2} H_n(\xi)$$

$$g_n^\Lambda(\eta) = (n!/(n+\Lambda)!)^{1/2} \eta^{\Lambda/2} L_n^\Lambda(\eta)$$

where  $H_n(\xi)$  and  $L_n^\Lambda(\eta)$  are the ordinary Hermite and Laguerre polynomials,

respectively.

The recursion relations for the polynomials  $h_n$  and  $g_n^\Lambda$  are:

$$h_{n+1}(\xi) = \left\{ \frac{1}{2}(n+1) \right\}^{-\frac{1}{2}} \xi h_n(\xi) - \left( \frac{n}{n+1} \right)^{\frac{1}{2}} h_{n-1}(\xi) \quad (5)$$

$$g_{n+1}^\Lambda(\eta) = \frac{(2n+\Lambda+1-\eta)}{[(n+1)(n+\Lambda+1)]^{\frac{1}{2}}} g_n^\Lambda(\eta) - \left[ \frac{(n+\Lambda)n}{(n+1)(n+\Lambda+1)} \right]^{\frac{1}{2}} g_{n-1}^\Lambda(\eta)$$

Now, the matrix elements  $B_{\beta\alpha}$ , can be calculated using the basis wave functions from Eq. (4). In the present model the spin-orbit force and the residual interactions are not included and the hamiltonian  $\mathcal{H}$  is simply a sum of the kinetic energy  $T$  plus the assumed single particle potential  $V = V(\rho, z) \equiv V(\xi, \eta)$ .

The kinetic energy matrix elements can be calculated analytically, and the only nonvanishing contributions are:

$$\begin{aligned} \langle n_z, n_\rho, \Lambda | T | n_z, n_\rho, \Lambda \rangle &= \frac{1}{2} \hbar \omega_\perp (2n_\rho + \Lambda + 1) + \frac{1}{2} \hbar \omega_z (n_z + \frac{1}{2}) \\ \langle n_z, n_\rho, \Lambda | T | n_z, n_{\rho+1}, \Lambda \rangle &= \frac{1}{2} \hbar \omega_\perp \{ (n_\rho + 1) (n_\rho + \Lambda + 1) \}^{\frac{1}{2}} \\ \langle n_z, n_\rho, \Lambda | T | n_{z+2}, n_\rho, \Lambda \rangle &= -\frac{1}{4} \hbar \omega_z \{ (n_z + 1) (n_z + 2) \}^{\frac{1}{2}} \end{aligned} \quad (6)$$

The potential energy matrix elements have to be calculated numerically:

$$\begin{aligned} \langle n'_z, n'_\rho, \Lambda' | V | n_z, n_\rho, \Lambda \rangle \\ = \delta_{\Lambda\Lambda'} \int_0^\infty d\eta \exp(-\eta) g_{n'_\rho}^\Lambda(\eta) g_{n_\rho}^\Lambda(\eta) \cdot Z_{n'_z n_z}(\eta) \end{aligned} \quad (7)$$

where:

$$Z_{n'_z n_z}(\eta) = \int_{-\infty}^\infty d\xi \exp(-\xi^2) h_{n'_z}(\xi) h_{n_z}(\xi) V(\xi, \eta) \quad (8)$$

From the recursion relations (5) one finds the recursion formula for the matrix elements  $Z_{n'_z, n_z}$

$$Z_{n'_z+1, n_z-1}^{(n)} = \left( \frac{n_z}{n'_z+1} \right)^{\frac{1}{2}} Z_{n'_z, n_z}^{(n)} - \left( \frac{n'_z}{n'_z+1} \right)^{\frac{1}{2}} Z_{n'_z-1, n_z-1}^{(n)} + \left( \frac{n_z-1}{n'_z+1} \right)^{\frac{1}{2}} Z_{n'_z, n_z-2}^{(n)} \quad (9)$$

For problems with reflection symmetry only the matrix elements between wave functions with the same parities are non-vanishing. This reduces substantially the size of the matrix B to be diagonalized. Furthermore, because of the relation (9) only the diagonal matrix elements need to be computed, all the others are obtained by recursions. In the cases with no reflection symmetry all the matrix elements are non-vanishing and must be calculated. Because of the recursion formulas only the computation of the diagonal and those adjacent to the diagonal matrix elements is actually necessary, all the others are obtained by recursion.

The integrals involved in formulas (7) and (8) have been done by the Gauss-Laguerre and Gauss-Hermite quadrature methods, using 14 and 32 mesh points in the  $\rho$  and  $z$  direction, respectively.

### The Time Dependent Schrödinger Equation

The time dependent equation is:

$$i\hbar \frac{\partial \psi_i(\vec{r}, t)}{\partial t} = \mathcal{H}_i(t) \psi_i(\vec{r}, t) \quad (10)$$

Inserting expansion (2), multiplying from the left by  $\phi_\beta^*$  and integrating one gets:

$$i\hbar \dot{a}_\beta^{(i)}(t) = \sum_\alpha B_{\beta\alpha}^{(i)} a_\alpha^{(i)} - i\hbar \sum_\alpha D_{\beta\alpha} a_\alpha^{(i)} \quad (11)$$

where:

$$B_{\beta\alpha}^{(i)} = \langle \phi_\beta | \mathcal{H}_i | \phi_\alpha \rangle$$

$$D_{\beta\alpha} = \langle \phi_\beta | \frac{\partial}{\partial t} | \phi_\alpha \rangle .$$

If the basis wave functions  $\phi_\alpha$  are time independent (fixed basis),  $D_{\beta\alpha} = 0$ , and the equation (11) simplifies to:

$$\dot{a}_\beta^{(i)} = (i\hbar)^{-1} \sum_\alpha B_{\beta\alpha}^{(i)} a_\alpha^{(i)} . \tag{12}$$

This is the first order differential equation for the time evaluation of the expansion coefficients  $a_\beta^{(i)}(t)$ . As  $a_\beta^{(i)}$  can be complex one can write  $a_\beta^{(i)} = X_\beta^{(i)} + i Y_\beta^{(i)}$ , and obtain a coupled system of differential equations for the real and imaginary parts of the coefficients  $a_\beta^{(i)}$ .

$$\dot{X}_\beta^{(i)} = \frac{1}{\hbar} \sum_\alpha B_{\beta\alpha}^{(i)} Y_\alpha^{(i)} \tag{13}$$

$$\dot{Y}_\beta^{(i)} = - \frac{1}{\hbar} \sum_\alpha B_{\beta\alpha}^{(i)} X_\alpha^{(i)} .$$

The equations (13) were solved numerically by an improved version of the predictor-corrector method<sup>18</sup> which is described below.

Let us denote by  $X_n$  and  $Y_n$  the values of  $X_\alpha^{(i)}$  and  $Y_\alpha^{(i)}$  at time  $t = n \cdot \Delta t$ .

First one calculates a predictor:

$$X_{n+1}^0 = X_{n-3} + \frac{4}{3} \Delta t (2\dot{X}_n - \dot{X}_{n-1} + 2\dot{X}_{n-2})$$

$$Y_{n+1}^0 = Y_{n-3} + \frac{4}{3} \Delta t (2\dot{Y}_n - \dot{Y}_{n-1} + 2\dot{Y}_{n-2})$$

where:

$$\begin{aligned} \dot{X}_n &= B_n Y_n / \hbar \\ \dot{Y}_n &= - B_n X_n / \hbar . \end{aligned} \tag{15}$$

Then modifies it to obtain:

$$\begin{aligned}\bar{X}_{n+1} &= X_{n+1}^0 + \frac{112}{121} (X_n - X_n^0) \\ \bar{Y}_{n+1} &= Y_{n+1}^0 + \frac{112}{121} (Y_n - Y_n^0).\end{aligned}\tag{16}$$

Finally one calculates:

$$\begin{aligned}\dot{\bar{X}}_{n+1} &= B_{n+1} \cdot \bar{Y}_{n+1}/h \\ \dot{\bar{Y}}_{n+1} &= - B_{n+1} \cdot \bar{X}_{n+1}/h\end{aligned}\tag{17}$$

and:

$$\begin{aligned}\tilde{X}_{n+1} &= \frac{1}{8} (9X_n - X_{n-2}) + \frac{3}{8} \Delta t (\dot{\bar{X}}_{n+1} + 2\dot{\bar{X}}_n - \dot{\bar{X}}_{n-1}) \\ \tilde{Y}_{n+1} &= \frac{1}{8} (9Y_n - Y_{n-2}) + \frac{3}{8} \Delta t (\dot{\bar{Y}}_{n+1} + 2\dot{\bar{Y}}_n - \dot{\bar{Y}}_{n-1}).\end{aligned}\tag{18}$$

The last step is to repeat (17) and (18) using  $\tilde{X}_{n+1}$  and  $\tilde{Y}_{n+1}$  just obtained.

The first four values at the points  $n = 0, 1, 2, 3$ , which are necessary to start the predictor-corrector procedure, are obtained by the Runge-Kutta method.

### SEQUENCE OF SHAPES

In order to provide some basis for comparison of this method with the classical hydrodynamical approach we choose a sequence of saddle to scission shapes for  $^{236}\text{U}$  that were calculated classically using a viscosity of  $0.02 \times 10^{12}$  poise.<sup>9,10</sup> This value of the viscosity was chosen to give the best agreement with the measured values of the asymptotic kinetic energy release for a wide range of nuclei.

The shapes themselves were parametrized in terms of smoothly joined portions of three quadratic surfaces of revolution. Figure 1 shows the parametrization. Table I lists the calculated values of  $\sigma_1$ ,  $\sigma_2$  and  $\sigma_3$  as a function of time and also gives the corresponding values of the potential energy of deformation  $E_V^0$ , the collective kinetic energy  $E_{\text{coll}}^0$  and the dissipated energy  $E_D^0$ . All of the shapes from Ref. 10 are axially symmetric, and also reflection symmetric. This sequence of shapes was obtained by starting the nucleus from its liquid drop model saddle point with 1 MeV of kinetic energy in the fission direction. For the value of viscosity chosen here the nucleus arrives at scission (a somewhat more elongated configuration than for the non-viscous case) in about  $38 \times 10^{-22}$  sec. These shapes were used for the single particle potential in our time dependent calculations of the microscopic energy of the system. In a later section we compare the values we obtained for the collective and dissipated energy with the hydrodynamic values.

In addition we made another calculation which required a slight generalization of the trajectory to include asymmetric shapes. Leaving the rest of the time development of the shape intact we introduced a difference in size between the two fragments that grew linearly in time so that the mass ratio at scission was 1.4 to 1 (which is approximately the

Table I. Hydrodynamical Calculations for the Fission of  $^{236}\text{U}$ . a)

$t$ ( $10^{-22}$ sec)	$\sigma_1$	$\sigma_2$	$\sigma_3$	$E_V^0$ (MeV)	$E_{\text{coll}}^0$ (MeV)	$E_d^0$ (MeV)
0.0	1.830	-0.0074	0.6376	4.5	1.0	—
5.5	2.215	-0.0604	0.6357	4.2	0.7	0.6
10.5	2.495	-0.1048	0.6422	3.6	0.9	1.0
15.5	2.807	-0.1472	0.6518	2.3	1.6	1.6
20.5	3.189	-0.1814	0.6618	- 0.1	3.1	2.5
25.5	3.649	-0.2042	0.6774	- 4.7	6.1	4.1
30.5	4.165	-0.2131	0.7024	-12.9	11.8	6.6
35.5	4.671	-0.2109	0.7418	-29.6	23.6	11.5
38.5	4.974	-0.2026	0.8009	-54.5	38.7	21.3

a) For the case  $\mu = 0.02$  terapoise given in Ref. 10.

value observed experimentally for the most probable division of this nucleus). Our goal was to investigate the dependence of the internal excitation energy on the mass asymmetry along the trajectory. There had been speculations that some of the apparent excitation of the nucleus along the original trajectory was connected with their reflection symmetry.<sup>19-21</sup> If a smaller amount of damping occurs along an asymmetric trajectory this could be associated with the preference of this nucleus for asymmetric division.

#### SINGLE PARTICLE POTENTIAL

For each shape along the specified trajectory a single particle well of the Woods-Saxon type is generated. We have used the procedure of Ref. 22 to insure that the normal diffuseness is approximately constant even for deformed shapes and we have chosen a diffuseness parameter  $a_v = 0.66$  fm ( $b_v = 1.20$  fm in the notation of Ref. 23). The radius (or scale) of the potential and its depth were chosen on the basis of Droplet Model considerations.<sup>24</sup> Figure 2 shows such a series of potentials for the case treated here. They extend from saddle toward scission and illustrate the approximate constancy of the normal diffuseness and the fact that the full well depth remains in the neck region even as one approaches scission. (One could compare these potentials with those in Fig. 1 of Ref. 25 which are calculated by a folding procedure which is probably more nearly correct.)

No spin-orbit term has been added as yet, and since we only consider neutrons in the preliminary calculations that have been done, there has been no need to include the Coulomb potential.



### ACCURACY OF THE METHOD

Because the adopted method of calculations is based on an expansion in a fixed harmonic oscillator basis we decided to check the dependence of the single particle energies on the number of oscillator shells in the basis. For the fixed basis the ratio  $\omega_1/\omega_2 = 4$  was chosen, which is the most appropriate basis for an intermediate shape between saddle and scission. The most crucial point therefore, was to check the behavior of the energy levels for the extreme shapes under investigation - the saddle point and scission shapes. In Fig. 3 the energies of the six levels  $M^\pi = 0^+$ , close to Fermi surface are presented as a function of the number of oscillator shells  $N$  in the basis. As one can see for  $N \geq 10$  the energies presented became stable, independent of  $N$ , for both shapes. In the calculations reported here  $N = 11$  was chosen and therefore one expects little error to result from this procedure.

The accuracy of the time dependent calculations was checked by calculating the norm of the time dependent wave functions  $N_t = | \langle \psi^i(r,t) \rangle |^2$ , which should be equal to 1. It turned out that the value  $N_t - 1$ , which was calculated, is always smaller than  $10^{-3}$ .

Another check was made by comparing the transition probabilities  $P$  for two levels coming close to each other to the Landau-Zener<sup>26</sup> expression.

$$P = \exp \left\{ - \frac{2\pi |\mathcal{H}'|^2}{\hbar |\dot{\alpha}(a-b)|} \right\} \quad (19)$$

where  $\mathcal{H}'$  is the perturbation which prevents levels from crossing<sup>27</sup> and is equal to one half of the energy difference between actual levels at the point of the closest approach. The quantity  $\dot{\alpha}$  is the speed at which

the shape of the potential changes and  $a$  and  $b$  are the slopes of the unperturbed energies (straight lines).

The calculations have been done for levels 4 and 5 belonging to the group  $M^\pi = 0^+$ , and levels 9 and 10 from the same group. The schematic situation for levels 4 and 5 is presented on Fig. 4 and the calculated probabilities in Table II.

In the Table II the Landau-Zener probabilities and those calculated here are presented in columns 3 and 4, respectively. The agreement, as one can see is very good. Obviously the numbers can not match perfectly, as the Landau-Zener expression applies to the idealized situation, where the influence of all other levels, except the two under consideration, is neglected. Therefore as should be expected the agreement for levels 4 and 5 is slightly better because of the lower density of levels in this region.

#### ENERGIES ASSOCIATED WITH THE MOTION

The results obtained in the damped hydrodynamic calculations<sup>9,10</sup> for the fission of  $^{236}\text{U}$  given in Table 1, indicate that of the 60 MeV that becomes available in the course of the motion (1 MeV of kinetic energy in the fission direction and 59 MeV from the saddle to scission change in potential energy) approximately 21.3 MeV is dissipated as a consequence of the viscosity assumed. Another 38.7 MeV appears as collective kinetic energy. The time development of these quantities is shown in Fig. 5. The dashed line indicates how the collective kinetic energy increases during the  $38.5 \times 10^{-22}$  sec. period necessary to move to scission. The solid line is obtained by adding the dissipated energy. (Both of these curves are scaled down by a factor of 144/236 so they can more

Table II. Comparison of Landau-Zener and Calculated Transition Probabilities

Level numbers $M^\pi=0^+$	$\dot{\alpha}$ ( $10^{-22}\text{sec}^{-1}$ )	$P_{L-Z}$	$P_{\text{calc}}$
4 and 5	0.175	0.27	0.25
	0.35	0.52	0.55
	0.7	0.73	0.77
	1.4	0.85	0.87
9 and 10	0.175	0.46	0.50
	0.35	0.68	0.70
	0.7	0.82	0.75
	1.4	0.91	0.83

easily be compared with the microscopic calculation which was done for the neutrons alone.)

For comparison with the collective kinetic energy found in the classical hydrodynamic calculation we calculated the microscopic quantity

$E_{\text{coll}}$ ,<sup>28</sup> where

$$E_{\text{coll}}(t) = \int \frac{1}{2} \rho \bar{v}^2 d\bar{r}. \quad (20)$$

The local flow velocity is calculated from the expression  $\bar{v} = \bar{j}/\rho$ . Where  $\rho$  and  $\bar{j}$  are, respectively, the quantum mechanical density and current defined by the expressions,

$$\rho(\bar{r}, t) = m \sum_i \Psi_i^* \Psi_i, \quad (21)$$

and

$$\bar{j}(\bar{r}, t) = \hbar \sum_i \text{Im}(\Psi_i^* \cdot \nabla \Psi_i), \quad (22)$$

where, the wave functions  $\Psi_i(\bar{r}, t)$  are solutions to the time dependent Schrödinger equation in the moving potential well. This definition has considerable intuitive appeal since it clearly applies to simple translations and would seem to give a reasonable result even for fairly turbulent flow. It breaks down, of course, when two components of the nuclear medium move against each other as in the case of the giant dipole resonance.

The values we calculated for  $E_{\text{coll}}$  all lie above the curve of hydrodynamic values in Fig. 5. This result might have been anticipated since the hydrodynamic calculations assume almost irrotational flow which yields the lowest possible kinetic energy. The microscopic calculations are presumably more turbulent.

The comparison of the dissipation energy in the two cases is not so straight forward. Because of the axial symmetry of the system the magnetic

quantum number  $m$  of a given level must remain the same in the course of the motion. The same is true for the parity  $\pi_z$  in the case of reflection symmetric shapes. Consequently, even if the motion of the potential is extremely slow (adiabatic) the system may end up in an excited state since there is no way for a particle to change to an empty level that moves down through the Fermi surface if its quantum numbers  $m$  and  $\pi_z$  are different from the levels being crossed. In our calculations a substantial part of the apparent excitation energy is of this type. This part of the energy  $E_s$  (where the subscript  $s$  indicates that it has its origin in symmetry effects) is simply the difference between the ground state of the system  $E_0$  (filling the lowest levels) and the "adiabatic" energy  $E_a$  (where the quantum numbers appropriate to the system are conserved.)

$$E_s = E_a - E_0 \quad (23)$$

$$E_0 = \sum_{i=1}^N E_i(\beta), \quad \text{lowest } N \text{ levels,} \quad (24)$$

$$E_a = \sum_{i=1}^N E_i(\beta), \quad \text{lowest } N \text{ levels having the} \quad (25)$$

appropriate quantum numbers.

In these expressions  $\beta$  is a one-dimensional deformation parameter measuring the distance along the dynamical path.

The total excitation energy  $E_t$  is defined as the difference between the total energy  $E^*$  of the system described by the time dependent Schrödinger equation and the ground state at that same value of  $\beta$ , where

$$E_t = E^* - E_0, \quad (26)$$

$$E^* = \sum_{i=1}^N E_i[\beta(t)], \quad (27)$$

and the  $E_i[\beta(t)]$  are the time dependent energy expectation values. Of course,  $E_t$

contains  $E_s$  (the apparent excitation arising purely from symmetry), as well as  $E_{\text{coll}}$ . If the motion is slow this is a serious defect that makes the calculation meaningless. If residual interactions were taken into account the system would always remain in its ground state for adiabatic changes in the potential well. The defect does not seem to be so serious in the case of rapid motion since the levels in a rapidly changing potential are more likely to retain their nodal structure (keeping  $m$  and  $\pi_z$  approximately the same) than to rearrange in order to follow a new level coming in from above.

In Fig. 5 both the total excitation energy  $E_t$  and that part arising from symmetry  $E_s$  are plotted against time for the two cases we have considered. One is the purely symmetric case (see Table I) and the other is a similar case where an asymmetry was gradually introduced along the trajectory so that the mass ratio was 1.4 to 1 at scission. The reason for comparing these two calculations was to determine whether the microscopic dynamics would give preference to asymmetric scission shapes as has often been speculated.<sup>19-21</sup> Indeed, the damping into intrinsic states is considerably less for the trajectory leading to an asymmetric mass division. However, the total excitation energy in both cases is so large (completely out of line with the experimental results or Liquid Drop Model predictions) as to raise serious questions about the validity of the approach.

## DISCUSSION

The results of this work serve to draw attention to the importance of single particle damping for large scale collective motion. They show that the energy dissipation profile is quite different than that associated with a hydrodynamic (or "two-body") viscosity. They also show (as has been frequently speculated) that asymmetric fission is preferred over symmetric fission on the basis of microscopic dynamical considerations. Another interesting result is that the microscopic collective kinetic energy is greater than that for irrotational flow indicating that some turbulence is generated by the collective motion. Consequently, we are inclined to question the applicability of the hydrodynamical saddle to scission trajectories. Both the dissipation and internal flow may well prefer a different sequence of shapes.

The main a priori objection to calculations of the type described here is their lack of self-consistency. Since the nuclear density distribution is simply driven forward by the predetermined motion of the potential well the system is manifestly non-conservative with regard to the total energy. Various prescriptions could be employed to keep the total energy approximately constant (such as adjusting the velocity along the trajectory)<sup>4</sup> but the lack of inherent self-consistency raises even more serious questions. If the nature of the damping provided by the excitation of intrinsic states can not be approximated by a hydrodynamic viscosity then not only is the rate of evolution of the potential well incorrect, but perhaps the sequence of shapes is incorrect as well.

In another study closely related to this one<sup>5</sup> an analytic expression has been derived for the energy absorbed by a classical gas of non-

interacting particles inside a container of fixed volume when the shape of the container changes. Of course, for adiabatic motion there is no change in internal energy. But by going to second order in the kinetic theory expansion one finds that for non-adiabatic motion of the container walls there is some internal excitation whose dependence on the changing shape of the container is quite different from that of a hydrodynamic viscosity.<sup>5-7</sup> Probably this type of damping (called "one-body" damping) is more nearly comparable to that which takes place in nuclei since an independent particle description certainly applies. Classical hydrodynamical calculations performed with this new type of damping give rise to a distinctly different sequence of shapes than those used here.<sup>8</sup> An important step in the continuation of this work would be to perform the microscopic calculations in potential wells following this new shape sequence to see if the damping along the path to scission is similar to the classical prediction.

Another defect of the model used here is the neglect of residual interactions. Their proper inclusion is expected to reduce the transition probabilities to higher levels, which would decrease the internal excitation. Calculations that have been done using the pairing interaction show considerably less damping,<sup>2</sup> but contain certain restrictions (designed to eliminate the collective part of the energy) that make some of the results questionable.

Our concern over the lack of self consistency in these calculations has lead us to consider Time Dependent Hartree-Fock (TDHF) as a natural extension of this work. The computational machinery developed here can be used as a basis for such calculations, and work along this line is now in progress.<sup>14</sup>



ACKNOWLEDGMENTS

We would like to thank W. J. Swiatecki for his stimulating interest and valuable discussions, Y. B. and J. B. would also like to thank N. K. Glendenning for the hospitality of the Nuclear Theory Group and the LBL-Nuclear Science Division for financial support during their stay in Berkeley.

FOOTNOTES AND REFERENCES

\* Work supported by the U. S. Energy Research and Development Administration.

† Present address: Nuclear Research Center-Negev, Beer-Sheva P.O.B. 9001, Israel; partially supported by an IAEA fellowship.

‡ Present address: Institute of Nuclear Research, 02-400 Swierke, Poland; partially supported by a Fulbright-Hays senior fellowship.

1. R. Wieczorek, R. W. Hasse and G. Süßmann, in "Proceedings of the Third International Atomic Energy Agency Symposium on Physics and Chemistry of Fission", Rochester, New York, 1973 (International Atomic Energy Agency, Vienna, 1974).
2. S. E. Koonin and J. R. Nix, Phys. Rev. C13, 209 (1976).
3. For example, see H. W. Schmidt, Arkiv for Fysik 36, 633 (1967) and references given there.
4. G. Schütte and L. Willets, in "Proceedings of the Third International Atomic Energy Agency Symposium on Physics and Chemistry of Fission", Rochester, New York, 1973 (International Atomic Energy Agency, Vienna, 1974).
5. W. J. Swiatecki, private communication.
6. W. J. Swiatecki, in Proceedings of the International School Seminar on Reactions of Heavy Ions with Nuclei and Synthesis of New Elements" Dubna, USSR (Oct. 1975).
7. J. Randrup, in the "Proceedings of the International Workshop IV on Gross Properties at Nuclei and Nuclear Excitation", Hirschegg, Austria (January 1976).
8. J. R. Nix and A. J. Sierk, private communication.

9. K.T.R. Davies, S. E. Koonin, J. R. Nix and A. J. Sierk, in the "Proceedings of the International Workshop III on Gross Properties of Nuclei and Nuclear Excitations", Hirschegg, Austria (January 1975) AED-Conf-75-009-000.
10. K.T.R. Davies, A. J. Sierk and J. R. Nix, Los Alamos Scientific Laboratory Report LA-UR-76-362 (February 1976).
11. T. Ledergerber, et al., Physics Lett. 56B, 417 (1975).
12. P. Bonche, S.Koonin and J. W. Negele, Phys. Rev. 18C (1975) in press.
13. P. Bonche, S. Koonin and J. W. Negele, Phys. Rev. C (in press); S. Koonin and J. W. Negele, separate papers in "The Proceedings of the International Workshop IV on Gross Properties of Nuclei and Nuclear Excitations," Hirschegg, Austria (January 1976).
14. J. P. Blocki and H. Flocard, private communication.
15. Y. Boneh, Z. Fraenkel and Z. Paltiel, In "Proceedings at the Third International Atomic Energy Agency Symposium on Physics and Chemistry of Fission", Rochester, New York, 1973 (International Atomic Energy Agency, Vienna, 1974).
16. Y. Boneh and Z. Fraenkel, Phys. Rev. C10, 893 (1974).
17. H. C. Pauli, Phys. Rep. 7C, 35 (1973).
18. R. W. Hamming, J. Assoc. Comp. Mach. 6, 37 (1959).
19. J. J. Griffin, Phys. Rev. Lett. 21, 826 (1968).
20. D. L. Hill and J. A. Wheeler, Phys. Rev. 89, 1102 (1953).
21. I. Kelson, Phys. Rev. Lett. 20, 867 (1968).
22. M. Brack et al., Rev. Mod. Phys. 44, 320 (1972).
23. W. D. Myers, Nucl. Phys. A204, 465 (1973).

24. W. D. Myers, Nucl. Phys. A145, 387 (1970).
25. M. Bosterli, E. O. Fiset and J. R. Nix, in "Proceedings of the Second IAEA Symposium on Physics and Chemistry of Fission", Vienna Austria, 1969 (International Atomic Energy Agency, Vienna, 1969).
26. C. Zener, Proc. R. Soc. A137, 696 (1932).
27. L. Willets, "Theories of Nuclear Fission", Clarendon Press, Oxford, 1964.
28. According to a suggestion of S. E. Koonin.
29. J. R. Nix, Nucl. Phys. A130, 241 (1969).

FIGURE CAPTIONS

Fig. 1. An illustration from Ref. 29 of a shape described by three smoothly joined portions of quadratic surfaces of revolution. Each surface is specified by the position  $\ell_i$  of its center, its transverse semiaxis  $a_i$  and its semisymmetry axis  $c_i$  (the quantity  $c_3$  is imaginary for this shape and hence not shown). The middle hyperboloid of revolution joins smoothly with the two end spheroids at  $z_1$  and  $z_2$ . The location  $\ell_{cm}$  of the center of mass of the drop is also shown. For reflection symmetric shapes, where  $a_1 = a_2 = a$  and  $c_1 = c_2 = c$ , three symmetric degrees of freedom can be defined by the expressions,

$$\begin{aligned}\sigma_1 &= (\ell_1 - \ell_1)/a, \\ \sigma_2 &= (a_3/c_3)^2 \\ \sigma_3 &= (a/c)^2.\end{aligned}$$

Fig. 2. The 10, 30, 50, 70 and 90 percent contours are shown for three shapes in the saddle to scission sequence used in the calculations described here. The algebraic method of Ref. 22 was used to create the diffuseness. Comparison with potentials generated by folding in a short-ranged function<sup>25</sup> show that there is considerable difference for the highly distorted shapes.

Fig. 3. The dependence of the single particle energies on the number of oscillator shells  $N$  used in the fixed basis. The solid lines correspond to the levels calculated at the saddle point, broken to those at scission.

Fig. 4. An illustration of the behavior of two levels at the point of closest approach. The solid lines represent the actually calculated energy levels, the broken ones their asymptotic behavior.

Fig. 5. The results of our microscopic calculations for the intrinsic excitation of the neutrons in  $^{236}\text{U}$  for a hydrodynamically<sup>10</sup> determined sequence of shapes from saddle to scission. The dashed line is the corresponding hydrodynamic collective kinetic energy (irrotational flow assumed) and the solid line is obtained by adding the internal energy arising from the viscous damping of the motion. The circles represent the results of our calculation for  $E_{\text{coll}}$  the collective kinetic energy,  $E_t$  the total excitation and  $E_s$ , which is that part of the total excitation connected with the symmetry of the potential. The triangles represent these same quantities in the case when reflection asymmetry is introduced.

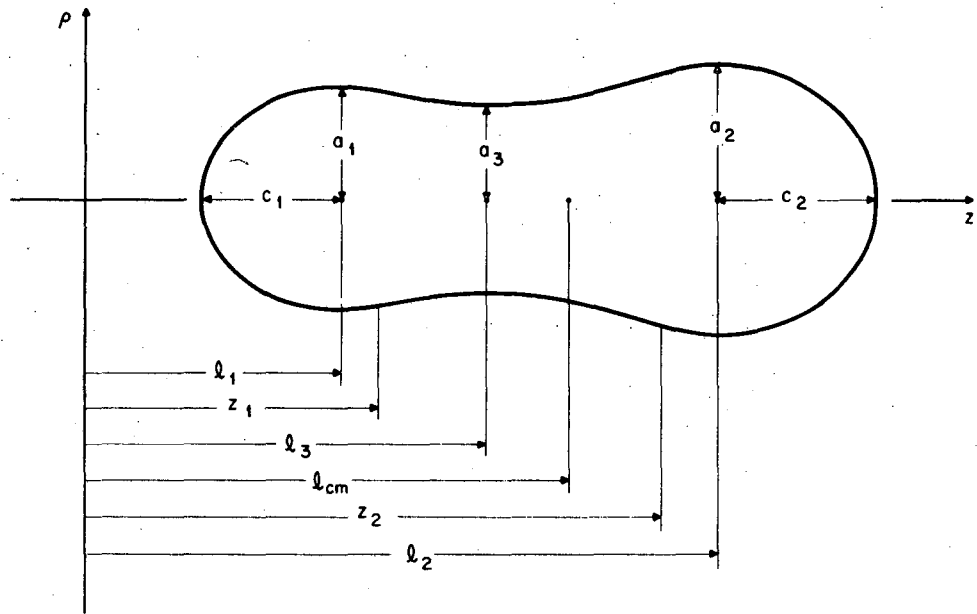


Fig. 1

XBL 678-3959 A

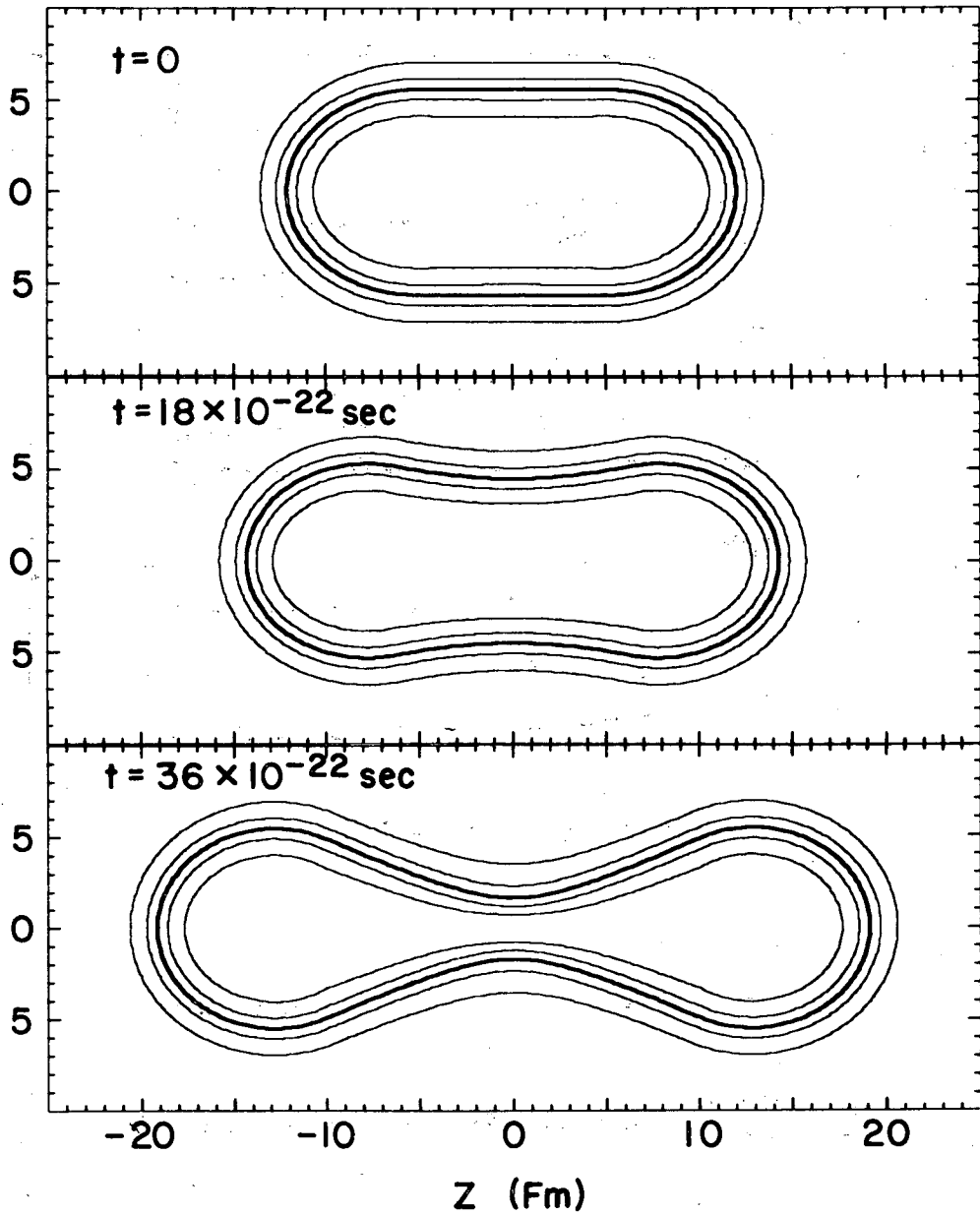


Fig. 2

XBL 763-2374

0 0 0 0 4 4 0 4 4 6 7



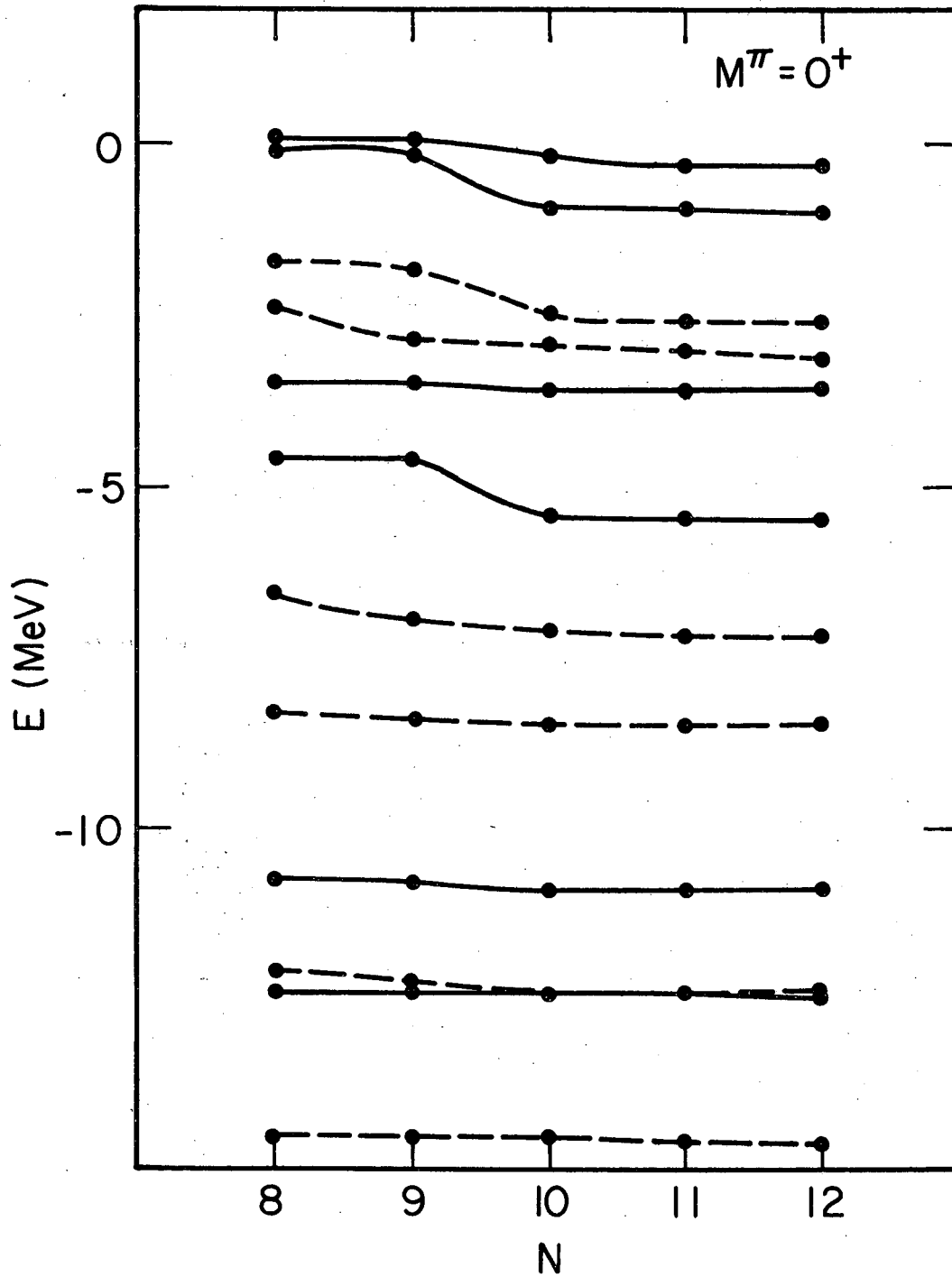


Fig. 3

XBL763-5237

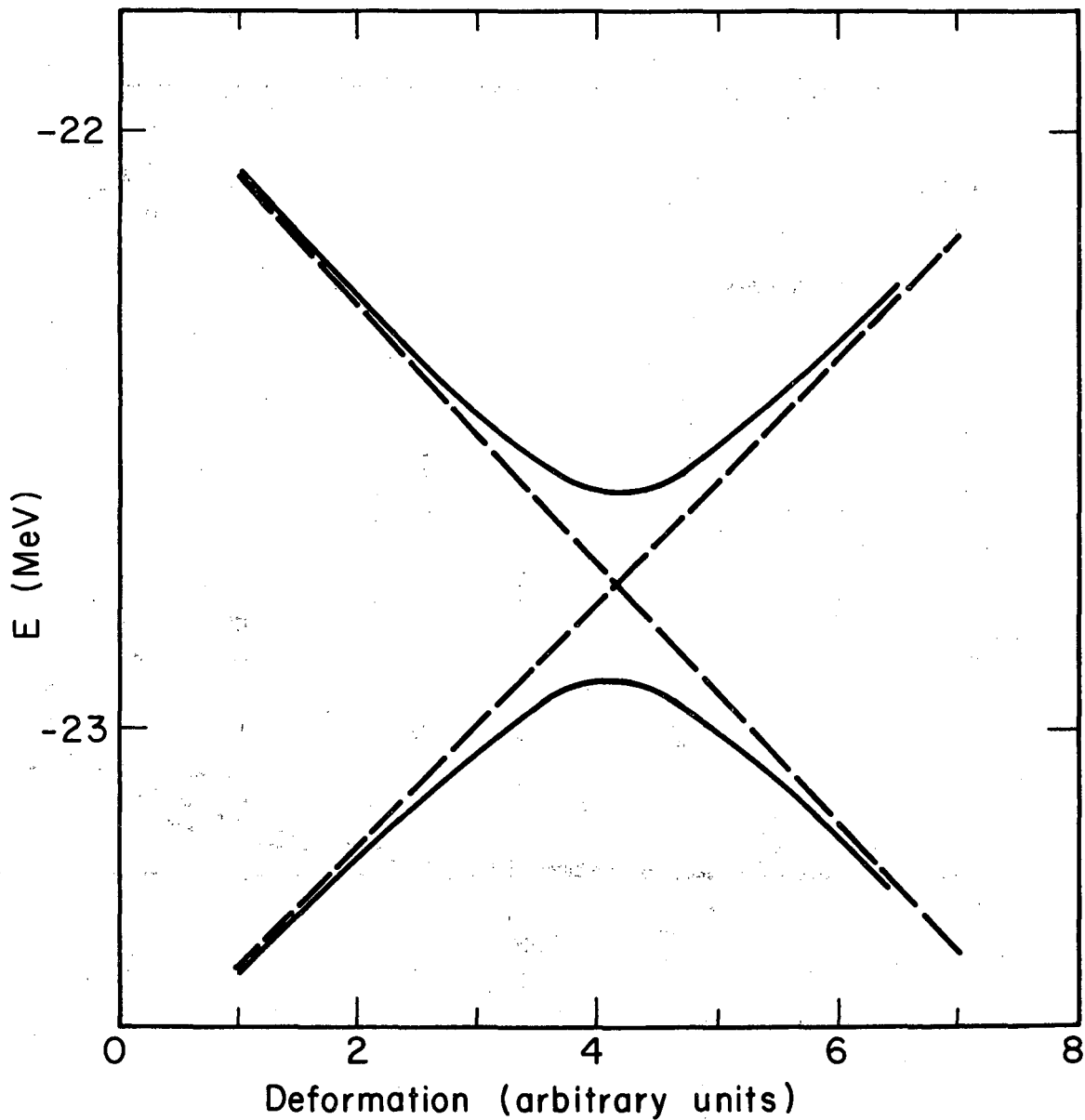


Fig. 4

XBL763-5238

0 0 0 0 4 4 0 4 4 6 8

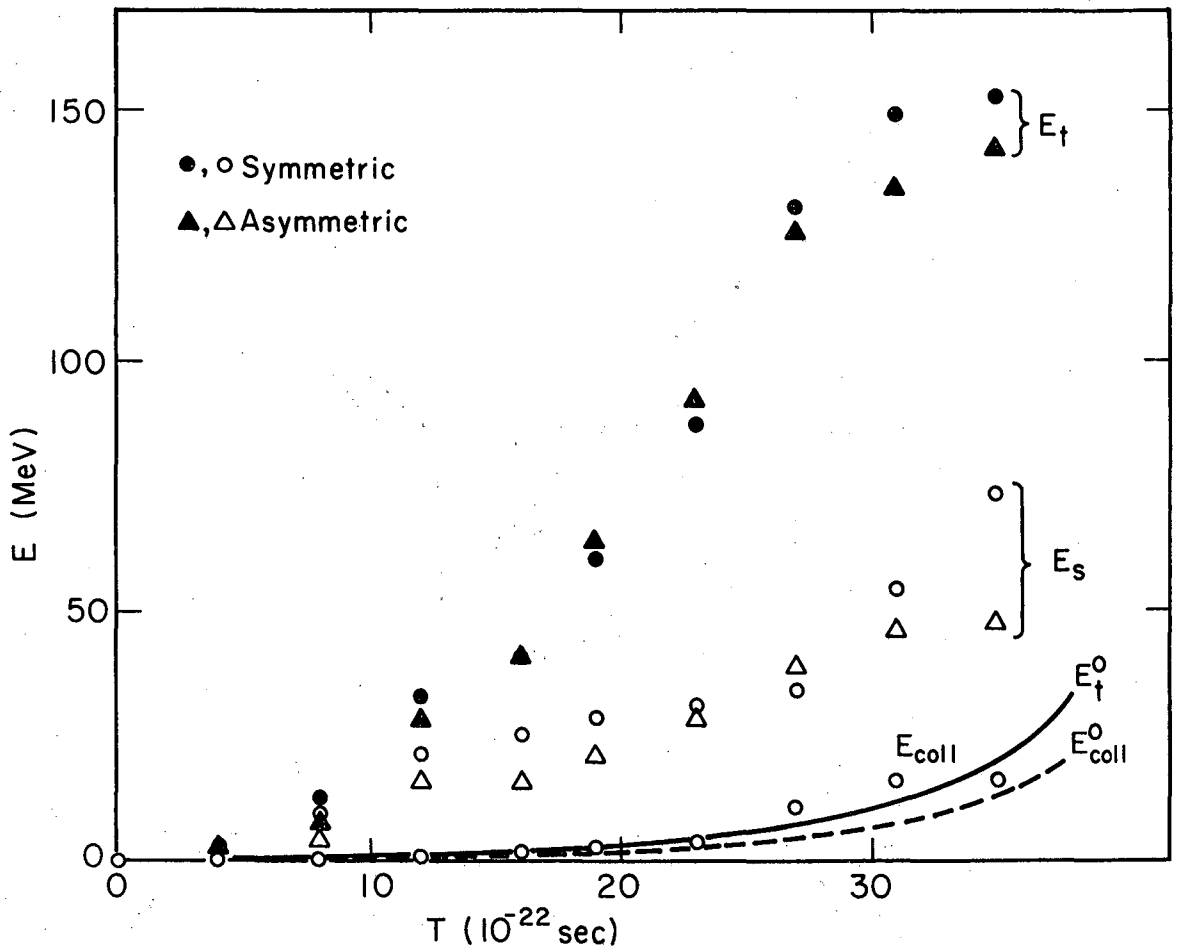


Fig. 5

XBL763-5239

**LEGAL NOTICE**

*This report was prepared as an account of work sponsored by the United States Government. Neither the United States nor the United States Energy Research and Development Administration, nor any of their employees, nor any of their contractors, subcontractors, or their employees, makes any warranty, express or implied, or assumes any legal liability or responsibility for the accuracy, completeness or usefulness of any information, apparatus, product or process disclosed, or represents that its use would not infringe privately owned rights.*

TECHNICAL INFORMATION DIVISION  
LAWRENCE BERKELEY LABORATORY  
UNIVERSITY OF CALIFORNIA  
BERKELEY, CALIFORNIA 94720